

LETTER • **OPEN ACCESS**

Intense agricultural irrigation induced contrasting precipitation changes in Saudi Arabia

To cite this article: Min-Hui Lo *et al* 2021 *Environ. Res. Lett.* **16** 064049

View the [article online](#) for updates and enhancements.

ENVIRONMENTAL RESEARCH
LETTERS

LETTER

Intense agricultural irrigation induced contrasting precipitation changes in Saudi Arabia

OPEN ACCESS

RECEIVED

18 February 2021

REVISED

19 April 2021

ACCEPTED FOR PUBLICATION

11 May 2021



PUBLISHED

28 May 2021

Original content from this work may be used under the terms of the [Creative Commons Attribution 4.0 licence](https://creativecommons.org/licenses/by/4.0/).

Any further distribution of this work must maintain attribution to the author(s) and the title of the work, journal citation and DOI.



Min-Hui Lo^{1,*} , Hao-Wei Wey¹, Eun-Soon Im^{2,*}, Lois Iping Tang^{1,3}, Ray G Anderson⁴, Ren-Jie Wu¹, Rong-You Chien¹, Jiangfeng Wei⁵, Amir AghaKouchak⁶ and Yoshihide Wada⁷ 

¹ Department of Atmospheric Sciences, National Taiwan University, Taipei, Taiwan

² Department of Civil and Environmental Engineering/Division of Environment and Sustainability, The Hong Kong University of Science and Technology, Hong Kong, People's Republic of China

³ Now at the Department of Earth and Planetary Sciences, Harvard University, Cambridge, MA, United States of America

⁴ USDA-ARS, US Salinity Laboratory, Agricultural Water Efficiency and Salinity Research Unit, Riverside, CA, United States of America

⁵ School of Atmospheric Sciences, Nanjing University of Information Science and Technology, Nanjing, People's Republic of China

⁶ Department of Civil and Environmental Engineering, and Department of Earth System Science, University of California, Irvine, CA, United States of America

⁷ International Institute for Applied Systems Analysis, Laxenburg, Austria

* Authors to whom any correspondence should be addressed.

E-mail: minhuilo@ntu.edu.tw and ceim@ust.hk

Keywords: Saudi Arabia, irrigation, water vapor convergence, decadal precipitation variations

Supplementary material for this article is available [online](#)

Abstract

Groundwater extraction has grown tremendously in Saudi Arabia to meet the irrigation water demand since the 1980s, and irrigation is one of the major anthropogenic factors modulating regional hydroclimate. However, the link between irrigation and hydroclimate is not well understood in a dry region such as Saudi Arabia. In this study, we utilize three different regional climate models to explore the physical mechanisms behind the irrigation impacts in this region. The results are robust across models and show that when irrigation is applied, wetter soil results in higher evapotranspiration and cools the lower atmosphere, leading to an anomalous pressure field and alters vapor transportation. Precipitation decreases locally because of the local cooling effect, whereas additional water vapor convergence enhances precipitation west to the irrigated region. This west–east contrast of precipitation change indicates a possible link between irrigation expansion in the 1980s and subsequent decadal precipitation variations in central Saudi Arabia. We further find from observations a decadal west–east contrast of precipitation changes in Saudi Arabia to support the similar finding in the models. This study implies the importance of including anthropogenic water management in climate models and provides a better understanding of how irrigation impacts local-to-regional climate.

1. Introduction

The Kingdom of Saudi Arabia (hereafter, Saudi Arabia) has a hot and dry climate, which limits productive rainfed agriculture (Elhadj 2004, DeNicola *et al* 2015). Precipitation ranges between 80 and 140 mm yr⁻¹, with 80% occurring during the wet season, November–April (Alkolibi 2002, Almazroui *et al* 2012). To support local agricultural production, Saudi Arabia has promoted irrigation projects in recent decades (Elhadj 2004, DeNicola *et al* 2015). In the early 1980s, wheat production increased as

a response to a self-sufficiency policy. Although the government has decreased wheat production since 1993 because of the high costs and environmental impacts, agricultural water usages remain high due to other agricultural products such as vegetables, fruits, and fodder crops (Elhadj 2004, Ouda 2014).

The irrigation hotspots are identified with census and remote sensing products. Figures 1(a) and S1 (available online at stacks.iop.org/ERL/16/064049/mmedia) show the spatial pattern of irrigation in Saudi Arabia (Food and Agriculture Organization of the United Nations 2009), and a belt of intensely

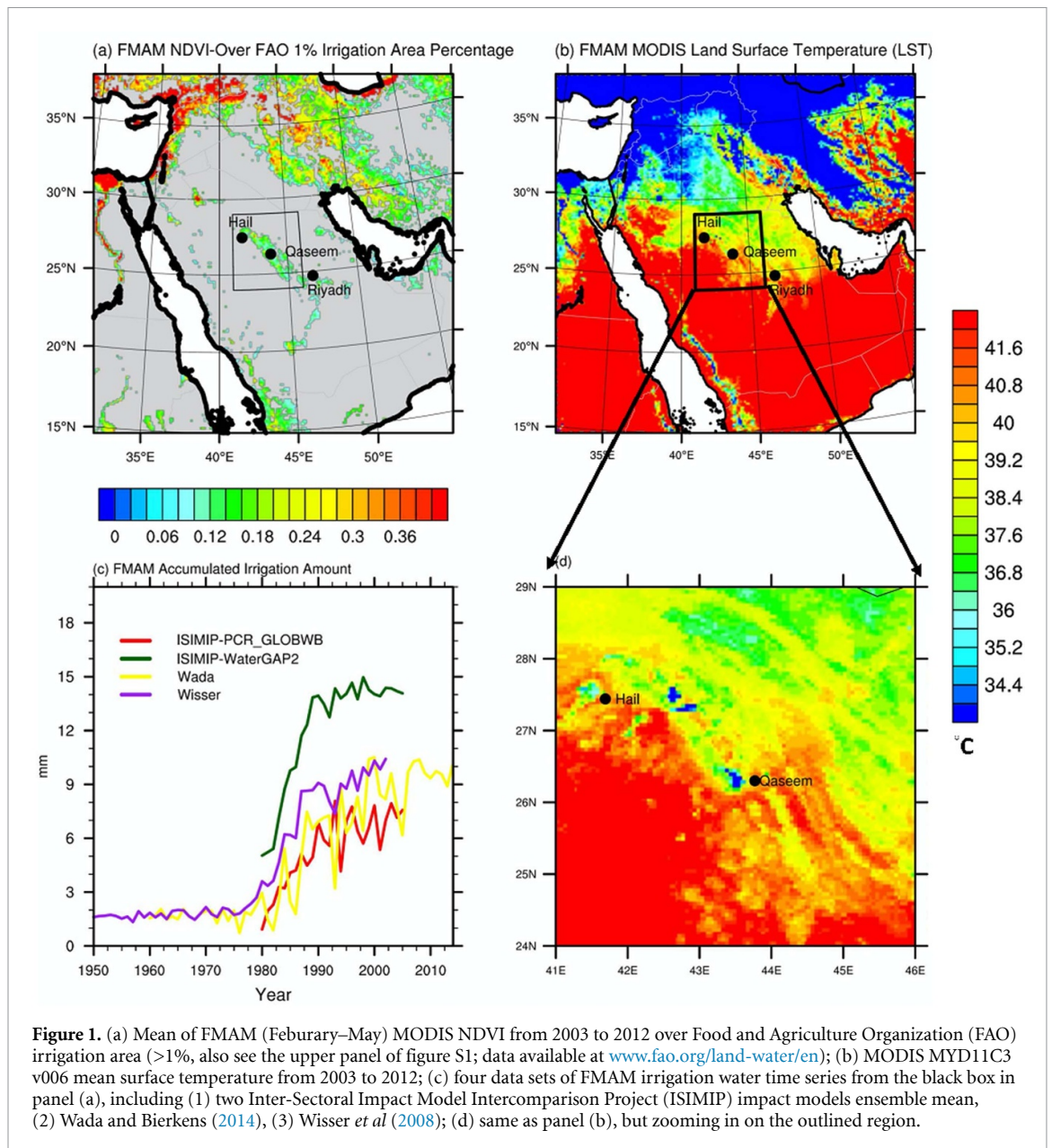
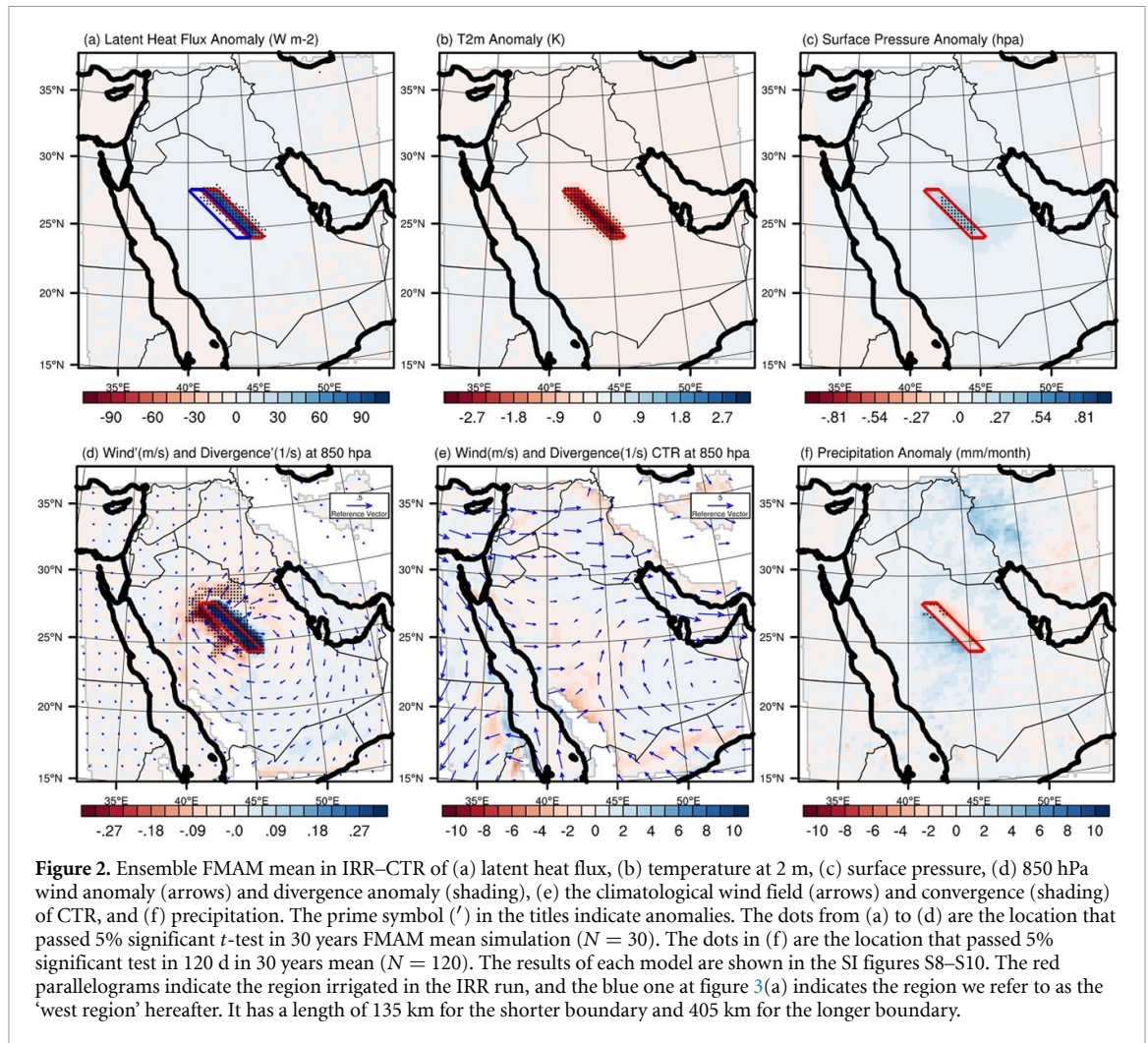


Figure 1. (a) Mean of FMAM (February–May) MODIS NDVI from 2003 to 2012 over Food and Agriculture Organization (FAO) irrigation area (>1%, also see the upper panel of figure S1; data available at www.fao.org/land-water/en); (b) MODIS MYD11C3 v006 mean surface temperature from 2003 to 2012; (c) four data sets of FMAM irrigation water time series from the black box in panel (a), including (1) two Inter-Sectoral Impact Model Intercomparison Project (ISIMIP) impact models ensemble mean, (2) Wada and Bierkens (2014), (3) Wisser *et al* (2008); (d) same as panel (b), but zooming in on the outlined region.

irrigated areas stretches across the central region of Saudi Arabia. The irrigation fingerprints are prominent in both land surface temperature (LST) and the normalized difference vegetation index (NDVI). From 2003 to 2012, the mean surface temperature (Wan *et al* 2015) in the irrigated region is over 2° cooler than the surroundings (figures 1(b) and (d)), and the NDVI (Didan 2015) is also correspondingly higher (figure S1, lower panel). The actual evapotranspiration rate is higher over the same region (Mahmoud and Gan 2019). These signals thereby demonstrate the strong regional hydroclimatic influences of irrigation. After the adoption of the self-sufficiency policy in the 1980s, the irrigation water demand increased abruptly by more than 100%, marking a sharp contrast (figure 1(c)) and has been rapidly depleting the groundwater reservoirs (Elhadj 2004).

With the changing intensity of irrigation, Saudi Arabia has a unique environment for investigating the impact of anthropogenic perturbations on the regional hydrological cycle and climate. The primary irrigation source for Saudi Arabia is nonrenewable groundwater (Elhadj 2004, Ouda 2014, DeNicola *et al* 2015), particularly over central Saudi Arabia. Previous work has investigated the impact of land modification (urbanization) on precipitation variability in Riyadh (Shepherd 2006). However, this study failed to find a conclusive link to urbanization. Instead, the study hypothesized a significant role for irrigation and recommended physically-based numerical simulations for future work (Shepherd 2006). Since rainfall in the wet season in Saudi Arabia is primarily convective, additional moisture provision through irrigation may influence atmospheric instability and further lead to precipitation changes. As such, in



this study, we utilize three different regional climate models to explore the potential impact of irrigation on regional precipitation in and near central Saudi Arabia.

2. Datasets and methods

Numerical models used in our study include the Weather Research and Forecasting (WRF) Model version 3.5.1 (Skamarock *et al* 2008), Regional Climate Model version 4 (RegCM4; Giorgi *et al* 2012), and Massachusetts Institute of Technology Regional Climate Model (MRCM; Im *et al* 2014b)—with a 27 km spatial resolution. The initial and boundary conditions for all the simulations are obtained from the European Centre for Medium-Range Weather Forecasts ERA-interim reanalysis data with a spatial resolution of 0.75° at 6 h intervals. The planetary boundary layer scheme is Yonsei University scheme for all the simulations. The WRF simulation employs the Noah Land Surface Model and Grell-Freitas ensemble convection scheme. The MRCM run uses the integrated biosphere simulator for the land surface scheme and Emanuel convection scheme.

RegCM4 is coupled to the biosphere-atmosphere transfer scheme and Tiedtke convection scheme. These schemes employed in the individual models are selected through various sensitivity experiments.

Three sets of irrigation water demand datasets (Wisser *et al* 2008, Wada and Bierkens 2014, Reyer *et al* 2019) are utilized; figure 1(c) shows the increases of irrigation water in the central Saudi Arabian (SA) from 1950 to 2010. The irrigated target area is set up as a northwest-southeast oriented parallelogram in Saudi Arabia (red parallelogram in figure 2). Two sets of idealized experiments are conducted: a control simulation without irrigation (CTR) and the other with idealized irrigation (IRR). For each model, the irrigation methods are applied differently by incorporating into different land surface schemes: for MRCM, the root zone (top 1 m of soil) is forced to field capacity, which is specified based on the observations of soil texture from the input data sets; for RegCM4, irrigation area does not allow the soil moisture to fall below the level of 60% of field capacity; for WRF, irrigation was simulated by holding soil moisture at 95% of porosity. If the consistent pattern of the

precipitation changes in response to irrigation water forcing could be found in spite of the usage of various irrigation schemes within structurally different land–surface models, it would help enhance the robustness of the model response.

The CTR simulations without additional surface moisture added aim to simulate the surface condition before 1980 when irrigation activities were not so widespread. Conversely, the IRR with moisture forcing imitates reality after 1980. In our irrigated region of interest, the land category, according to the default setting by USGS land use categories in WRF, is mostly shrubland (59 grids out of 75 grids), with barren or sparsely vegetated being the second majority (15 grids out of 75 grids).

All the simulations are done for 4 months in each of the 30 years from 31 January 1982 to 31 May 2011. The corresponding ERA-interim data are used for the initialization, and the result at the end of May would not influence the initialization of February in the next year. Considering the overlapping time of the wet season and irrigation season of our objective, the period of February–May is chosen. The domain, as shown by figure 1(a), includes most parts of the Arabian Peninsula and the Red Sea with part of the East Mediterranean and the Persian Gulf. Although the irrigated area is set up with a 405 km long and 135 km wide parallelogram, the location and extent roughly correspond to the irrigation region provided by the FAO of the United Nations (2009) (figure 1(a)). The irrigated area, which is designed as the shape of a red parallelogram (figure 2(a)), is approximately 51 030 km². The amount of supplied water for irrigation varies yearly and according to irrigation schemes employed in different RCMs (i.e. WRF, RegCM4, MRCM).

For observational data, monthly total rainfall in central Saudi Arabia from Yearbook by the [General Authority for Statistics](#) of Kingdom of Saudi Arabia (www.stats.gov.sa/en/46) is employed to investigate the precipitation changes. Three stations in central Saudi Arabia are chosen for this analysis: Hail (27.44° N, 41.69° E), Qaseem (26.30° N, 43.77° E), and Riyadh (24.71° N, 46.73° E) (figures 1(a) and (b)). Among the rain gauge stations in Saudi Arabia, these are the only stations located close to our region of interest and have data before 1980 available (see figure 1 in Athar (2015) for the map of the meteorological stations). Following Athar (2015), we also employed a similar method for the quality control on the precipitation data (SI and figure S2). The observational data indicate that February–May (FMAM) is the intersection of irrigation water application and wet season (figure S5). Two rain gauge-based gridded precipitation products—Global Precipitation Climatology Center (GPCC; Schneider *et al* 2011) and Multi-Source Weighted-Ensemble Precipitation (MSWEP; Beck *et al* 2019)—and a satellite-derived precipitation

product—Global Precipitation Climatology Program (GPCP; Adler *et al* 2003)—are also used for model precipitation verification. Data version for GPCP and GPCC are v2.2 and v6, respectively. The spatial resolutions are 2.5°, 1°, and 0.1° for GPCP, GPCC, and MSWEP, respectively. For temperature, we use the Climatic Research Unit (CRU; Harris *et al* 2014) data. Further details and figures for model verification are available in the supplementary information (figures S6 and S7). For a given time series in this study, its mean's statistical significance is determined based on a student *t*-test with a null hypothesis that the difference is zero. We then calculate its *p*-value.

3. Results

3.1. Model results

Before we focus on the model response to irrigation, the basic performance of three model's CTR simulations are evaluated. The surface temperature and precipitation in CTR (from 30 years of average) are comparable to those of the observation-based datasets, including the CRU (Harris *et al* 2014), GPCC (Schneider *et al* 2011), GPCP (Adler *et al* 2003), and MSWEP (Beck *et al* 2019) (figures S6 and S7). While we show here the ensemble mean for the sake of simplicity, the results are robust across models (SI).

Since irrigation can modulate regional climate (e.g. Guimberteau *et al* 2001, Kueppers *et al* 2007, Sacks *et al* 2009, Ozdogan *et al* 2010, Puma and Cook 2010, Harding *et al* 2012, Lo *et al* 2013, Im and Eltahir 2014, Im *et al* 2014b, Sorooshian *et al* 2014, Fowler *et al* 2018), crucial components in the hydroclimatic cycle (i.e. the rainfall amount, intensity, and frequency; evapotranspiration rate or latent heat fluxes; sensible heat fluxes; near-surface atmospheric variables, such as water vapor, temperature, and pressure; local atmospheric circulation) may change due to the surface cooling and moistening of soil from irrigation water. The simulated difference between IRR and CTR (IRR–CTR based on 30 years average) is shown in figure 2, which uncovers physical mechanisms. The strong responses of relevant variables are mostly appeared in and around red parallelogram in figure 2(a), where irrigation forcing is given to the model, which roughly corresponds to the actual irrigation region seen from remote sensing observations (figure 1(a)). For the direct effect of irrigation, the latent heat flux is more than 50 W m⁻² larger in the irrigated region (figure 2(a)). The increase in latent heat flux further lowers the 2 m temperature by more than 2K (figure 2(b)). The magnitude of simulated cooling is consistent with the observation. As a result of the cooler lower atmosphere, an anomalous high surface pressure develops (figure 2(c)). The high-pressure system is associated with a descending anomaly, which corresponds to an

Table 1. Effects of irrigation on the irrigated region and the west region in the mean from three models at 1982–2011 FMAM (IRR – CTR). Boldface values indicate statistically significant differences at $p < 0.05$.

Variable (anomaly)	Units	Irrigation	West of irrigation
Latent heat flux	W m^{-2}	79.34	20.9
T2m	K	−2.67	−0.99
Surface pressure	hPa	0.29	0.17
Divergence	$\text{s}^{-1} \times 10^5$	0.48	−0.14
Precipitation	mm month^{-1}	−1.36	3.15

anomalous local divergence in the lower atmosphere (figure 2(d)).

Despite the anomalous local divergence, an increase in convergence exists just west to the irrigated region, which triggers changes in rainfall. This convergence is related to the climatological wind field. Anomalous westerly winds occur east of the irrigated region, and easterly winds occur to the west due to the pressure field. The anomalous easterly wind converges (figure 2(d)) with the climatological westerly winds (figure 2(e)), which favors the convergence to the west of the irrigated region (the blue box in figure 2(a)). The enhancement of convergence is also associated with an increase in rainfall (figure 2(f)), which is about $3.48 \text{ mm month}^{-1}$ (13%) more than the control run (figure S16). The pattern of rainfall anomaly highly corresponds with the convergence anomaly pattern, which is a contrast change of rainfall increases to the west and decreases locally in the irrigated region (figure 2(f)). This further implies the importance of dynamic factors such as wind convergence to the enhancement of rainfall, in addition to changes in moisture amount. The anomalous values (IRR–CTR) of the domain averages for the irrigated region and the west region are also shown in table 1.

Further insights are provided by looking at the occurrence number of rainfall events at different intensities (figure 3). In the irrigated region, the IRR run (figure 3(a)) shows an overall decrease in the occurrence of precipitation at different intensities. On the contrary, the western region (figure 3(b)) shows a general increase in the number of events for all rainfall intensities. By further digging into the time of occurrence, we found the precipitation anomalies tend to happen when rainfall events already exist. The 15 d mean CTR and (IRR–CTR) precipitation time series in the irrigated region and immediately west of the irrigated area are shown in figure S17. The anomalous precipitation in the western area is mostly positive. These positive rainfall anomalies tend to happen when rain already occurs. In other words, the irrigation activity may

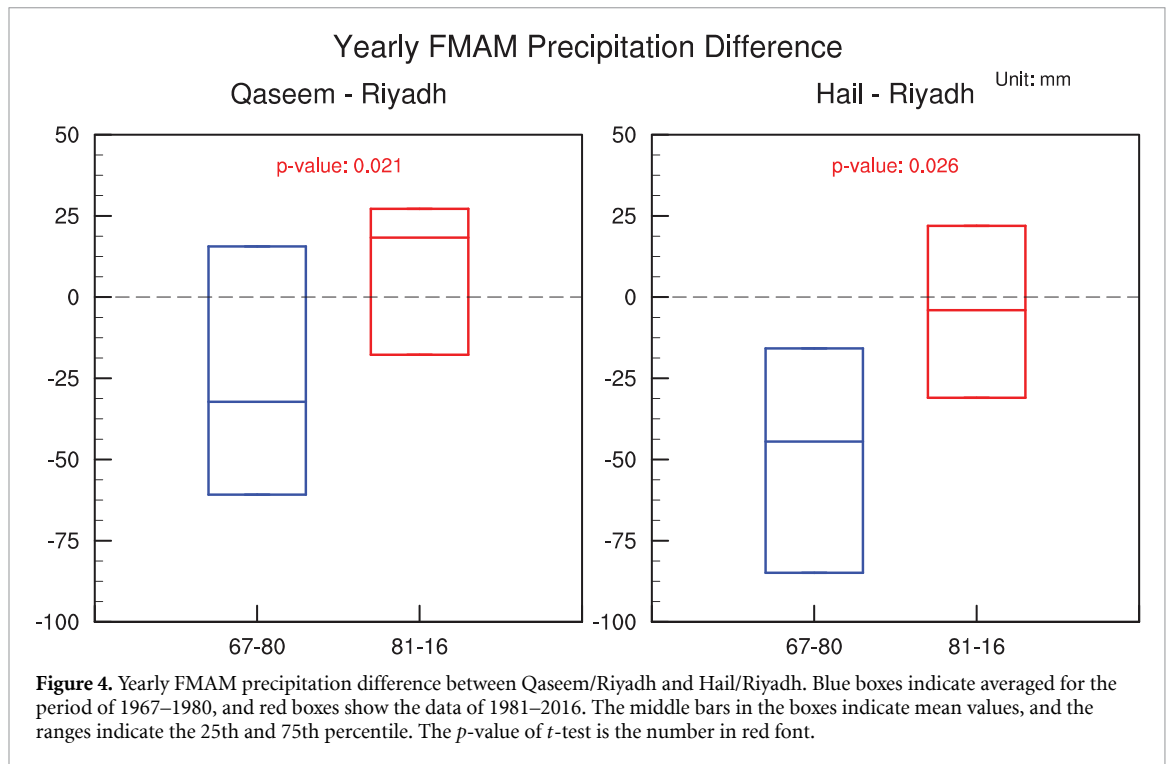
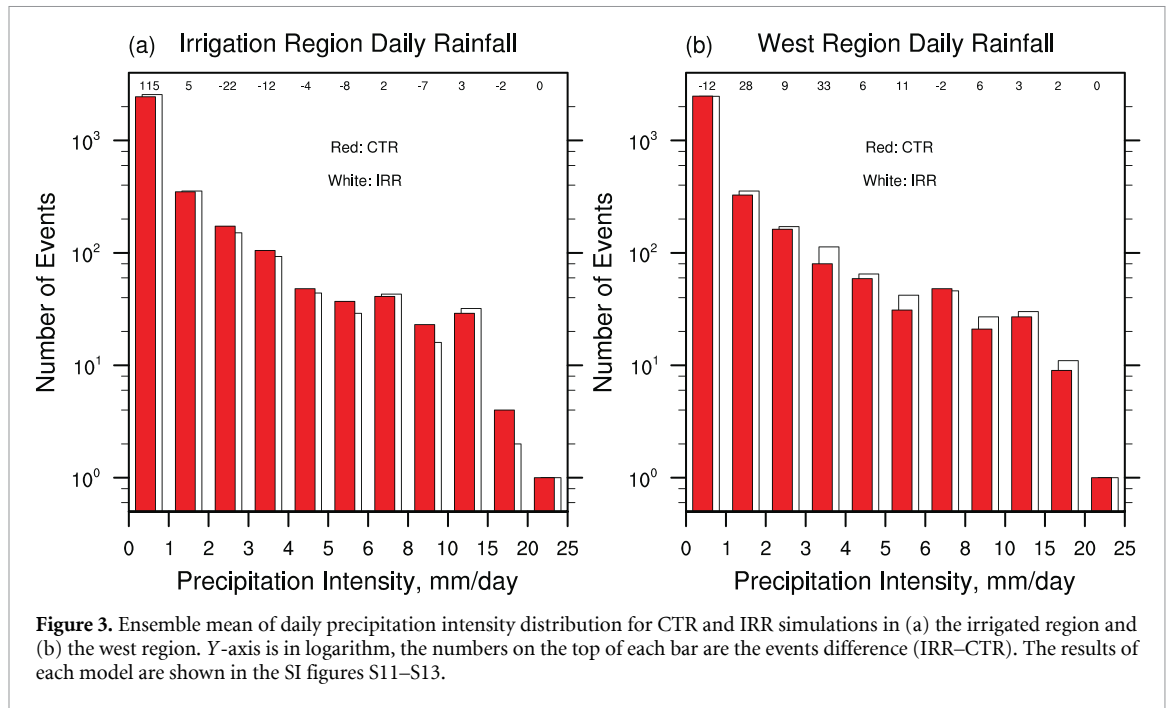
intensify existing rain events instead of creating new ones.

3.2. Suggestive information from observations

Extensive irrigation in central Saudi Arabia has impacted the regional hydroclimate. This irrigation comes from nonrenewable, deep fossil, groundwater formed at least 20 000 years ago with a negligible recharge rate (FAOUN 2009). Despite the unsustainable usage, observed precipitation of the three stations in central Saudi Arabia showed a marginal increase from 1980 to 2016 compared to the period of 1967–1978. We chose three rain gauge stations close to the heavily irrigated region of central Saudi Arabia—Hail, Qaseem, and Riyadh (figures 1(a) and S3a)—to evaluate the observed effect of irrigation on precipitation. While the separate precipitation time series of the three stations do not indicate significant trends from 1967–2016 (figure S3(b)), their west–east differences indicate changes of precipitation anomalies from the period of 1967–1980 to the 1981–2016 (figure 4).

The precipitation contrast is calculated from differences between the two stations west of the major irrigation region (Hail and Qaseem) and the one to the east (Riyadh). Figure 4 shows the precipitation contrast between Qaseem/Riyadh and Hail/Riyadh before and after 1980. Other time periods have been tested but this did not affect the results (figure S3(c) and SI). Compared to Riyadh, precipitation at both Hail and Qaseem significantly increased (p -value < 0.025) after the growth of irrigation in the early 1980s. This suggests an increase in rainfall in the stations on the west side relative to the east side among the three stations close to the irrigated region. In addition, multi-model simulations illustrate how this increase in precipitation can occur. The potential for this extra precipitation to increase groundwater recharge needs further investigation. However, the necessary observations to validate these changes are limited. While this study used idealized simulations, the models should consider more realistic irrigation amounts and the sub-grid heterogeneity for future research.

Previously, the influences of irrigation in precipitation in desert environments were uncertain due to competing effects (van Heerwaarden *et al* 2009). The increase in latent heat flux is counteracted by reduced atmospheric instability due to surface cooling. A theoretical framework suggests wet soil conditions favor enhanced precipitation, implying the dominance of the increased latent heat flux (Eltahir 1998). In contrast, observational and modeling studies focusing on irrigation mostly suggest suppressed rainfall over the irrigated region, thus supporting the dominance of the increased atmospheric stability from the surface cooling effect (Douglas *et al* 2009, Im *et al* 2014b, Pei *et al* 2016). This cooling effect also dominates the



decreased precipitation over the irrigated region of this study.

Along with local rainfall suppression, the increase in rainfall might occur elsewhere, such as downwind (Harding and Snyder 2012, Pei et al 2016) or other nearby regions (Lo and Famiglietti 2013, Alter et al 2015a, 2015b), and even remote, non-adjacent regions (Wei et al 2013, de Vrese et al 2016). Here, the enhanced precipitation occurs in the upwind region. During the springtime (March–May), the rainfall in central Saudi Arabia is often associated

with the westerly from the Mediterranean depressions (Hasanean et al 2015). This prevailing wind direction also favors the irrigation effect on the west side of the study region. Thus, the enhancement of precipitation largely depend on where the anomalous convergence is, which can result from the combined effects by the local circulation changes and the mean environmental circulation. There is usually a divergence anomaly in the local irrigation regions because of cooling-induced high surface pressure and anti-cyclonic circulation. This anti-cyclonic circulation

interacts with the prevailing wind (which is the westerly in this study), causing an anomalous convergence in the west of the irrigation regions, which is the upwind region enhancement as shown in this study. However, some studies (e.g. DeAngelis *et al* 2010, Lo and Famiglietti 2013, Im *et al* 2014b, Alter *et al* 2015a, Zhang *et al* 2017) approached this problem by considering the contrasting nature of soil wetting: surface cooling from evaporation versus the moistening effect from increased atmospheric humidity. Usually, the surface cooling can make irrigated areas less favorable for convection due to reduced sensible heat, and instead irrigation-induced precipitation primarily occurs on the downwind side with more extra water vapor that has been transported from irrigated areas.

4. Conclusions and discussion

This study highlights the importance of human-driven impacts on the hydrological cycle and regional climate in central Saudi Arabia. The contribution of irrigation to changes in rainfall patterns can be seen from the limited observations (figure 4 and SI). Idealized model simulations support the finding in observational data and further provide an insight into the physical processes involved (figures 2 and 3). The analysis from ensemble simulations shows that irrigation leads to a spatial change in the anomalous precipitation field: rainfall west to the irrigated region increases by about $3.48 \text{ mm month}^{-1}$ (13%), while it decreases locally by about $1.42 \text{ mm month}^{-1}$ (5%). Note that another irrigation experiment using the FAO irrigation area and several years of WRF cloud-resolving scale simulation are also conducted with somewhat consistent results (figures S14, S15 and SI). Note that figure S19 presents the irrigation water amount (rectangular bar) for 4 months (i.e. from February to May) with interannual variability (error bar) with respect to three models. While MRCM requires roughly 500 mm per 4 months period, the WRF and RegCM4 experiments have much more water, reaching over 800 mm per 4 months period. Seemingly, it is a huge amount compared to the precipitation amount in that region. However, this study does not intend to make any specific conclusion for the actual practice of irrigation. Instead, the nature of the study is highly theoretical, and the objective is to understand the robust physical mechanism that emerges, regardless of the modeling system used. A substantial water forcing benefits to amplify the model response. This study shows how precipitation and related dynamics can be influenced by surface irrigation, which implies the importance of including anthropogenic water management in climate models for regional hydrological and climate dynamics to be simulated realistically. In addition, modeling and quantifying the effect of irrigation should be done within the framework of climate change experiments. This study

thus underscores the importance of including anthropogenic water management in climate models so that regional hydrological and climate dynamics can be simulated reasonably.

Saudi Arabia serves as one of the leading examples of climate change and water resource issues (DeNicola *et al* 2015), and agriculture in Saudi Arabia is vulnerable to changes in temperature and precipitation (Alkolibi 2002, Chowdhury *et al* 2013). A previous study estimated the water table in Saudi Arabia to decrease at a rate of 0.181 m yr^{-1} until 2050, and the increasing temperature will lead to further demand in agricultural water usage (Chowdhury and Al-Zahrani 2013). The water supplies in Saudi Arabia are estimated to be gone in 5 decades (DeNicola *et al* 2015) at current and forecasted rates of consumption. Currently, part of the water demand in Saudi Arabia is satisfied by other water sources such as desalinated water and treated wastewater (DeNicola *et al* 2015). Thus, a better understanding of how irrigation impacts local-to-remote climate and water availability is essential for improving water management under ongoing climate change circumstances because global warming will intensify the hydrological cycle and resultant rainfall characteristics in any kind of way (IPCC 2013).

Data availability statement

Two irrigation water demand datasets are based on Wada and Bierkens (2014) and Wisser *et al* (2008). The spatial irrigation intensity dataset is based on the FAO, which can be obtained from www.fao.org/land-water/en. For the observational monthly precipitation datasets, we use GPCP version 6 (www.esrl.noaa.gov/psd/data/gridded/data.gpcp.html) and GPCC (<https://psl.noaa.gov/data/gridded/data.gpcp.html>).

For Saudi Arabia station rainfall data, we use General Authority for Statistics from Kingdom of Saudi Arabia at www.stats.gov.sa/en/46. For the observational monthly precipitation gridded datasets, GPCC precipitation data were provided by the NOAA/OAR/ESRL PSD, Boulder, Colorado, USA, from their website at www.esrl.noaa.gov/psd/. For MSWEP, the data were from www.gloh2o.org/. GPCP were provided by the NOAA/OAR/ESRL PSD, Boulder, Colorado, USA, from their website at www.esrl.noaa.gov/psd/. For CRU surface temperature data, the data were provided by <https://crudata.uea.ac.uk/cru/data/hrg/>. The NDVI and LST data were from the Terra/aqua/MODIS Daily L3 Global 0.05 Deg. CMG dataset was acquired from the Level-1 and Atmosphere Archive and Distribution System (LAADS) and Distributed Active Archive Center (DAAC), located in the Goddard Space Flight Center in Greenbelt, Maryland (<https://ladsweb.nascom.nasa.gov/>).

The data that support the findings of this study are available upon reasonable request from the authors.

Acknowledgments

This study was supported by the Ministry of Science and Technology in Taiwan under Grant 106-2111-M-002-010-MY4. Eun-Soon Im was supported by the Hong Kong Research Grants Council funded project (GRF16309719). We specially thanks Dr Matthew McCabe's and Miss Tzu-Ying Wu's comments on this study and Dr Ahmed Kenawy for providing the observational rainfall datasets in Saudi Arabian region.

Author contributions

The paper was conceived and written by M-H L, H-W W, E-S I, and Y W, A A, R A, and L T provided comments and discussed with M-H L. Three regional climate models are conducted and analyzed by R-J W, R-Y C, E-S I, J W processed the moisture tracking data and discussed with M-H L on the results.

Conflict of interest

The authors declare no competing interests.

Code availability statement

The code that supports the findings of this study is available from the corresponding authors on request.

ORCID iDs

Min-Hui Lo  <https://orcid.org/0000-0002-8653-143X>

Yoshihide Wada  <https://orcid.org/0000-0003-4770-2539>

References

- Adler R F *et al* 2003 2 global precipitation climatology project (GPCP) monthly precipitation analysis (1979–present) *J. Hydrometeorol.* **4** 1147–67
- Alkolibi F M 2002 Possible effects of global warming on agriculture and water resources in Saudi Arabia: impacts and responses *Clim. Change* **54** 225–45
- Almazroui M, Islam M N, Jones P D, Athar H and Rahman M A 2012 Recent climate change in the Arabian Peninsula: seasonal rainfall and temperature climatology of Saudi Arabia for 1979–2009 *Atmos. Res.* **111** 29–45
- Alter R E, Fan Y, Lintner B R and Weaver C P 2015a Observational evidence that Great Plains irrigation has enhanced summer precipitation intensity and totals in the midwestern United States *J. Hydrometeorol.* **16** 1717–35
- Alter R E, Im E-S and Eltahir E A B 2015b Rainfall consistently enhanced around the Gezira scheme in East Africa due to irrigation *Nat. Geosci.* **8** 763–7
- Athar H 2015 Teleconnections and variability in observed rainfall over Saudi Arabia during 1978–2010 *Atmos. Sci. Lett.* **16** 373–9
- Beck H E, Wood E F, Pan M, Fisher C K, Miralles D G, van Dijk A I J M, McVicar T R and Adler R F 2019 MSWEP V2 global 3-hourly 0.1° precipitation: methodology and quantitative assessment *Bull. Am. Meteorol. Soc.* **100** 473–500
- Chowdhury S and Al-Zahrani M 2013 Implications of climate change on water resources in Saudi Arabia *Arab. J. Sci. Eng.* **38** 1959–71
- de Vrese P, Hagemann S and Claussen M 2016 Asian irrigation, African rain: remote impacts of irrigation *Geophys. Res. Lett.* **43** 3737–45
- DeAngelis A, Dominguez F, Fan Y, Robock A, Kustu M D and Robinson D 2010 Evidence of enhanced precipitation due to irrigation over the Great Plains of the United States *J. Geophys. Res.* **115** D15115
- DeNicola E, Aburizaiza O S, Siddique A, Khwaja H and Carpenter D O 2015 Climate change and water scarcity: the case of Saudi Arabia *Ann. Global Health* **81** 342–53
- Didan K 2015 MYD13C2 MODIS/aqua vegetation indices monthly L3 global 0.05Deg CMG V006 [Data set]. NASA EOSDIS land processes DAAC (<https://doi.org/10.5067/MODIS/MYD13C2.006>)
- Douglas E M, Beltrán-Przekurat A, Niyogi D, Pielke Sr R A and Vörösmarty C J 2009 The impact of agricultural intensification and irrigation on land–atmosphere interactions and Indian monsoon precipitation—a mesoscale modeling perspective *Glob. Planet. Change* **67** 117–28
- Elhadj E 2004 Camels don't fly, deserts don't bloom: an assessment of Saudi Arabia's experiment in desert agriculture *Occasional Pap.* **48** 6
- Eltahir E A 1998 A soil moisture–rainfall feedback mechanism: 1. Theory and observations *Water Resour. Res.* **34** 765–76
- Food and Agriculture Organization of the United Nations 2009 *Rome Groundwater Management in Saudi Arabia Draft Synthesis Report*
- Fowler M D, Pritchard M S and Kooperman G J 2018 Assessing the impact of indian irrigation on precipitation in the irrigation-enabled community earth system model *J. Hydrometeorol.* **19** 427–43
- General Authority for Statistics n.d. (available at: www.stats.gov.sa/en/46)
- Giorgi F, Coppola E and Solmon F 2012 Mariotti L and others RegCM4: model description and preliminary tests over multiple CORDEX domains *Clim. Res.* **52**
- Guimberteau M, Laval K, Perrier A and Polcher J 2001 Global effect of irrigation and its impact on the onset of the Indian summer monsoon *Clim. Dyn.* **39** 1329–48
- Harding K J and Snyder P K 2012 Modeling the atmospheric response to irrigation in the Great Plains. Part I: general impacts on precipitation and the energy budget *J. Hydrometeorol.* **13** 1667–86
- Harris I, Jones P, Osborn T and Lister D 2014 Updated high-resolution grids of monthly climatic observations—the CRU TS3.10 Dataset *Int. J. Climatol.* **34** 623–42
- Hasanean H and Almazroui M 2015 Rainfall: features and variations over Saudi Arabia, a review *Climate* **3** 578–626
- Im E S and Eltahir E A 2014 Enhancement of rainfall and runoff upstream from irrigation location in a climate model of West Africa *Water Resour. Res.* **50**
- Im E S, Gianotti R L and Eltahir E A 2014a Improving simulation of the West African monsoon using the MIT regional climate model *J. Clim.* **27** 2209–29
- Im E S, Marcella M P and Eltahir E A 2014b Impact of potential large-scale irrigation on the West African monsoon and its dependence on location of irrigated area *J. Clim.* **27** 994–1009
- IPCC 2013 Summary for policymakers *Climate Change 2013: The Physical Science Basis. Contribution of Working Group I to the Fifth Assessment Report of the Intergovernmental Panel on Climate Change* ed T F Stocker, D Qin, G-K Plattner, M Tignor, S K Allen, J Boschung, A Nauels, Y Xia, V Bex and P M Midgley (Cambridge: Cambridge University Press)

- Kueppers L M, Snyder M A and Sloan L C 2007 Irrigation cooling effect: regional climate forcing by land-use change *Geophys. Res. Lett.* **34**
- Lo M H and Famiglietti J S 2013 Irrigation in California's central valley strengthens the southwestern US water cycle *Geophys. Res. Lett.* **40** 301–6
- Mahmoud S H and Gan T Y 2019 Irrigation water management in arid regions of Middle East: assessing spatio-temporal variation of actual evapotranspiration through remote sensing techniques and meteorological data *Agric. Water Manage.* **212** 35–47
- Ouda O K M 2014 Impacts of agricultural policy on irrigation water demand: a case study of Saudi Arabia *Int. J. Water Resour. Dev.* **30** 282–92
- Ozdogan M, Rodell M, Beaudoin H K and Toll D 2010 Simulating the effects of irrigation over the United States in a land surface model based on satellite-derived agricultural data *J. Hydrometeorol.* **11** 171–84
- Pei L, Moore N, Zhong S, Kendall A D, Gao Z and Hyndman D W 2016 Effects of irrigation on summer precipitation over the United States *J. Clim.* **29** 3541–58
- Puma M and Cook B 2010 Effects of irrigation on global climate during the 20th century *J. Geophys. Res.* **115** 1–15
- Reyer C et al 2019 ISIMIP2b simulation data from biomes sector. GFZ data services (<https://doi.org/10.5880/PIK.2019.012>)
- Sacks W J, Cook B I, Buening N, Levis S and Helkowski J H 2009 Effects of global irrigation on the near-surface climate *Clim. Dyn.* **33** 159–75
- Schneider U, Becker A, Finger P, Meyer-Christoffer A, Rudolf B and Ziese M 2011 GPCP full data reanalysis version 6.0 at 0.5°: monthly land–surface precipitation from rain-gauges built on GTS-based and historic data (https://doi.org/10.5676/DWD_GPCC/FD_M_V7_050)
- Shepherd J M 2006 Evidence of urban-induced precipitation variability in arid climate regimes *J. Arid Environ.* **67** 607–28
- Skamarock W C, Klemp J B, Dudhia J, Gill D O, Barker D M, Duda M G, Huang X-Y, Wang W and Powers J G 2008 A description of the advanced research WRF version 3. NCAR Tech. Note NCAR/TN-475+STR 113
- Sorooshian S et al 2014 Influence of irrigation on land hydrological processes over California *J. Geophys. Res.* **119** 13137–52
- van Heerwaarden C C, Vilà-Guerau de Arellano J, Moene A F and Holtslag A A 2009 Interactions between dry-air entrainment, surface evaporation and convective boundary-layer development *Q. J. R. Meteorolog. Soc.* **135** 1277–91
- Wada Y and Bierkens M F 2014 Sustainability of global water use: past reconstruction and future projections *Environ. Res. Lett.* **9** 104003
- Wan Z, Hook S and Hulley G 2015 MYD11C3 MODIS/Aqua Land Surface Temperature/Emissivity Monthly L3 Global 0.05° CMG V006 [Data Set]. NASA EOSDIS Land Processes DAAC
- Wei J, Dirmeyer P A, Wisser D, Bosilovich M G and Mocko D M 2013 Where does the irrigation water go? An estimate of the contribution of irrigation to precipitation using MERRA *J. Hydrometeorol.* **14** 275–89
- Wisser D, Frohling S, Douglas E M, Fekete B M, Vörösmarty C J and Schumann A H 2008 Global irrigation water demand: variability and uncertainties arising from agricultural and climate data sets *Geophys. Res. Lett.* **35** L24408
- Zhang X, Xiong Z and Tang Q 2017 Modeled effects of irrigation on surface climate in the Heihe River Basin, Northwest China *J. Geophys. Res.: Atmos.* **122** 7881–95